1. INTRODUCTION

1.1. Photosynthesis

This chapter summarizes important aspects of the mechanisms that lead to O_2 formation in Photosystem II (PSII). After a brief introduction to the structure and function of the PSII complex, the S-state cycle is outlined and the structure and oxidation states of the catalytic Mn_4Ca complex are summarized. On that basis, current information concerning disassembly and photoassembly processes are reviewed. The states, binding, and location of the distinct intermediates involved in dis- and reassembly paths are discussed. Finally, the aims of this works are delineated.

Solar energy capture and conversion into chemical energy and biopolymers by photoautotrophic organisms are the basis for respiration life on Earth. A broad range of organisms have developed a complex molecular machinery for the efficient conversion of sunlight to chemical energy over the past 3 billion years, which to the present day has not been matched by any man-made technologies.

As it fundamentally changed the redox balance on earth and permitted development of aerobic metabolism and more-advanced life forms (Blankenship, 2001). The development of oxygenic photosynthesis was one of the most important events in earth's history. Oxygenic photosynthesis is likely an early event which developed during evolution 3.5 billion years ago. The key in oxygenic photosynthesis is the development of the manganese complex that is capable of water oxidation.

Photosynthesis is one of the most important biological processes on earth. It converts solar energy into chemical energy (Blankenship, 2002). Most photosynthetic organisms release molecular oxygen into the atmosphere. Through water oxidation, they generate chemical energy in the form of ATP and reducing power in the form NADPH, which are then used to reduce CO_2 and to produce carbohydrates.

The total photosynthetic activity in the biosphere consumes 1.5×10^{22} J/year of light energy. This is only a small fraction (0.05 %) of the total light energy arriving on the surface of the earth (about 3×10^{24} J/year). From this energy input, about 200 billion tons of biomass are produced through photosynthetic organisms per year, thereby fixing more than 10 % of the total atmospheric CO_2. The carbohydrates formed by this process serve as food for all

living organisms (for reviews on photosynthesis see (Blankenship, 2001; Blankenship, 2002; Kruse et al., 2005)).

The empirical equation representing the net reaction of photosynthesis for oxygen-evolving organisms can be written as:

$$6CO_2 + 12H_2O \xrightarrow{h\nu} C_6H_{12}O_6 + 6O_2 + 6H_2O \qquad \text{[Eq 1]}$$

The standard free energy for the synthesis of glucose is + 2.870 kJ/mol.

This simple reaction is the sum of two processes. In the light reactions, water is oxidized, forming di-oxygen (O_2). The electrons from this process are used to reduce $NADP^+$, whereas the pumping of protons across a lipid bilayer membrane creates an electrochemical gradient that provides the energy for ATP synthesis. In the dark reactions, ATP is consumed in a reaction where NADPH is used to reduce carbon dioxide, forming glucose and other carbohydrates (Lehninger et al., 2000).

1.1.1 Oxygenic Photosynthetic Organisms

The photosynthetic process in all plants and algae as well as in certain types of photosynthetic bacteria involves the removal of electrons from H_20, which results in the release of O_2. In this process, known as oxygenic photosynthesis, water is oxidized by the photosystem II (PSII) reaction center, a multisubunit protein located in the photosynthetic membrane. Decades of research have shown that the structure and function of PSII is similar in plants, algae and cyanobacteria, so that knowledge gained in one species can be applied to others (Whitmarsh and Govindjee, 1999).

1.1.2 Oxygenic Photosynthesis

The energy conversion in eukaryotes (plants and algae) takes place in the thylakoid membrane located inside of the chloroplasts.

The chloroplasts are small organelles (5-10 μm in diameter and 2-4 μm thick) found inside specialized leaf cells. They are surrounded by a double-membrane envelope and contain the thylakoid membrane system. Photosynthetic pigment-protein complexes, which absorb light and transfer electrons and protons, are located in the thylakoid membrane (Figure 1). The protein complexes embedded in the photosynthetic membrane are oriented with respect to the inner and outer phase to allow creating an electrochemical gradient of protons across the thylakoid membrane.

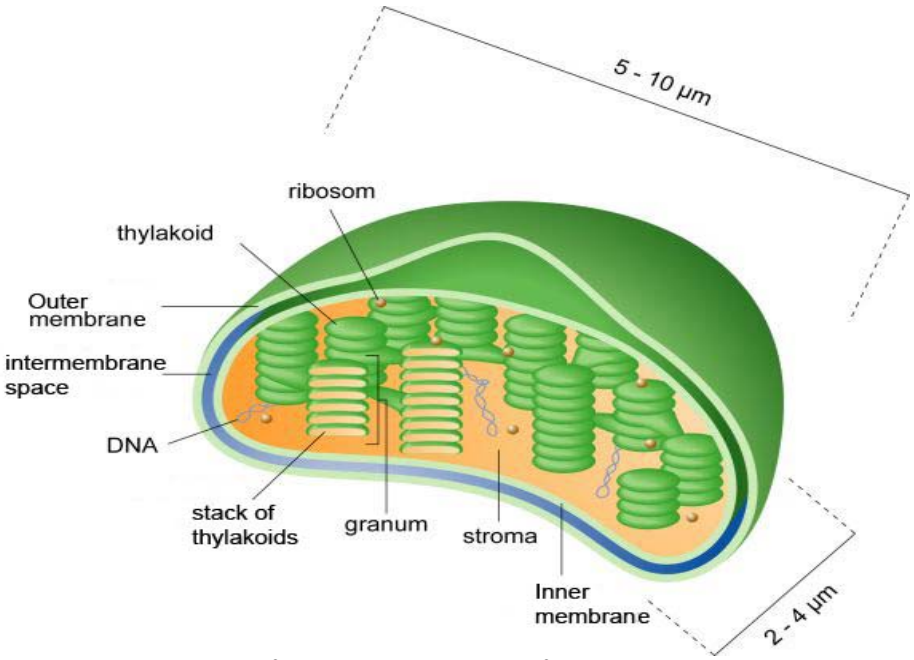

Figure 1 Schematic picture of the overall organization of the membranes in the chloroplast. The region of the chloroplast that is inside the inner membrane but outside the thylakoid membranes is the stroma. It contains the enzymes that catalyze carbon fixation and other biosynthetic pathways. The thylakoid membranes are highly folded and appear to be stacked like coins; they form one or a few large interconnected membrane systems, with a well-defined interior and exterior with respect to the stroma. The inner space within a thylakoid is denoted as lumen (www.vscht.cz).

The overall arrangement of the photosynthetic protein complexes in the membrane is shown in Figure 2. After initial light excitation and charge separation in PSII, the oxidised primary donor $P680^{\bullet+}$ oxidises via a redox active Tyr the nearby Mn-cluster located at the lumenal side. This cluster in turn catalyses the oxidative cleavage of water into four protons and molecular oxygen.

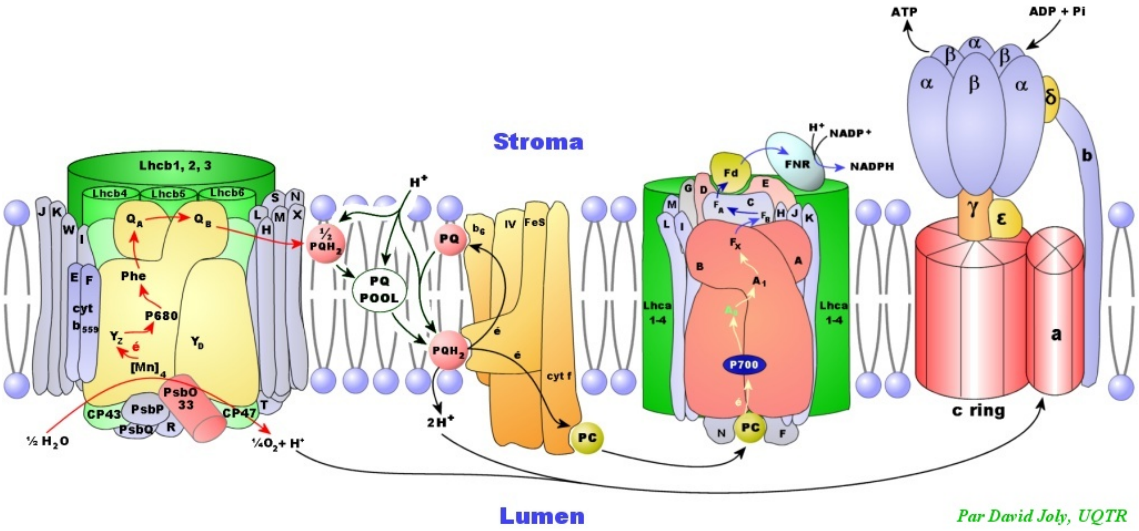

Figure 2 A schematic representation of functional organization of the protein complexes which couple photosynthetic electron transport to the transport of protons across the thylakoid membrane, the synthesis of ATP, and the reduction of NADPH showing the main components of its electron transport chain. Reprinted from http://www.uqtr.ca/labcarpentier/eng/research.htm.

The final electron acceptor of PSII, a plastoquinone molecule named Q_B, leaves the complex at the stromal side as plastoquinol after the uptake of two protons and two electrons. PSII can be described as a water-plastoquinone-oxidoreductase, catalysing the following reaction:

$$2H_2O + 2PQ + 4H^+_{stromal} \xrightarrow{4h\nu} O_2 + 2PQH_2 + 4H^+_{lumenal}\,.$$

In the linear electron transport, all three complexes (PSI, PSII, Cyt b_6f) are connected in series, and the electron transfer processes in and between the three complexes can be visualized in the so called Z-scheme (Figure 3). Here, PSII is shown as the functional unit transferring electrons from water to the plastoquinone (PQ) acceptor that in turn donates electrons via the Cyt b_6f complex to PSI (Govindjee and Krogmann, 2004).

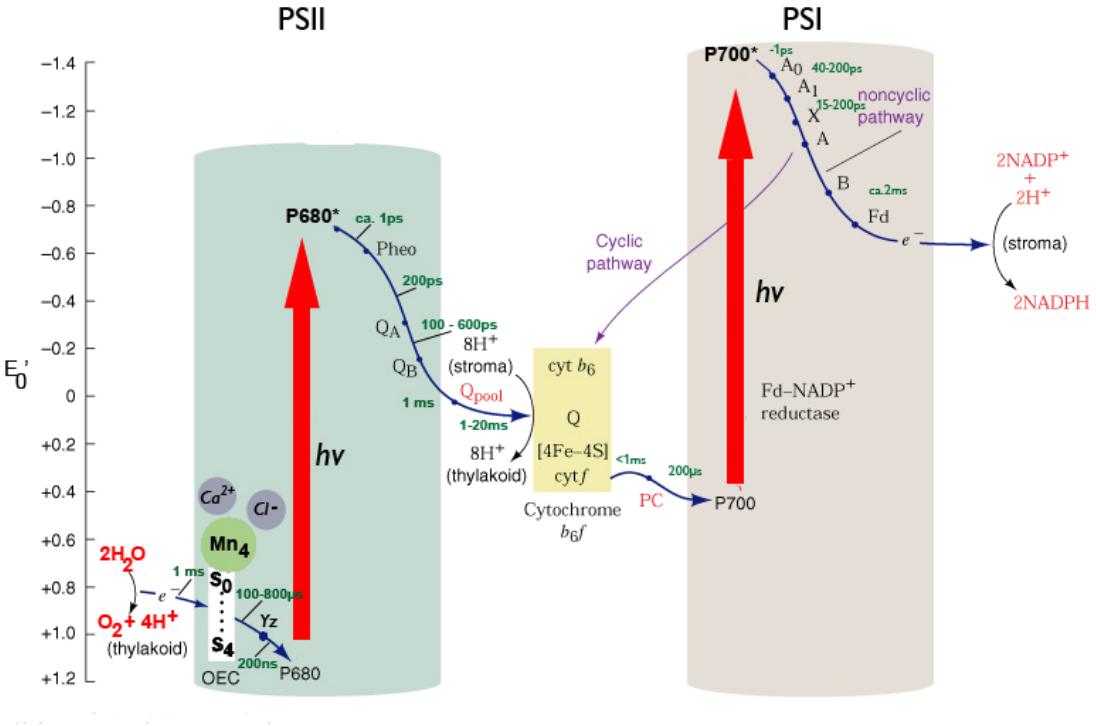

Figure 3 The Z-Scheme is a representation of photosynthetic electron flow from H_2O to $NADP^+$. The energy relationships can be derived from the E_0' scale beside the Z diagram, with lower standard potentials and hence greater energy (from bottom to top). Energy input as light is indicated by two broad arrows, P680* and P700* represent photoexcited states. Electron loss from P680* and P700* creates $P680^+$ and $P700^+$. The representative components of the three supramolecular complexes (PSI, PSII, and the cytochrome b_6/cytochrome f complex) are in shaded boxes enclosed by solid red lines. Proton translocations which establish the proton-motive force driving ATP synthesis are illustrated as well. Adapted from (Satoh et al., 2005).

1.2 Photosystem II

1.2.1 Organization of Photosystem II

Highlighting the complexity of this process, the study of the photosynthetic apparatus is a prime example of research that requires a combined effort between numerous disciplines, including quantum mechanics, biophysics, biochemistry, molecular and structural biology, as well as physiology and ecology. The time courses that are measured in photosynthetic reactions range from femtoseconds to days.

Photosystem II (PSII) is found in higher plants, algae and cyanobacteria and is highly conserved among these organisms. It exists as a homodimer and the total molecular weight is approximately 650 kDa. Each monomer contains up to 20 protein subunits and diverse cofactors which are found either intrinsic or extrinsic to the lipid bilayer. PSII consist of a reaction center that carries out the conversion of light energy to stable chemical energy, and an antenna system carrying chlorophylls and carotenoids that harvests light and transfers the energy to the reaction center. The reaction center (RC) core contains two homologous transmembrane proteins known as D1 and D2, which bind cofactors facilitating the primary charge separation (Barber, 2002; Nixon et al., 2005). Closely associated with the D1 and D2 proteins are two chlorophyll-containing proteins named CP43 and CP47. They are also structurally homologous, each having six transmembrane α-helices. Finally, the PSII RC core complex has several extrinsic proteins attached to its lumenal surface which shield the water oxidizing site from too intimate contact with solutes present in the aqueous phase (Seidler, 1996; De Las Rivas et al., 2004; Bricker and Burnap, 2005).

The PSII RC core complex is serviced by peripheral light-harvesting systems, which vary among different organisms (Green and Durnford, 1996; Green and Gantt, 2005). In plants and green algae, this antenna system is intrinsic and composed of LHC proteins that bind Chla and Chlb, whereas in cyanobacteria and red algae, phycobilins arranged within the extrinsically located phycobilisomes carry out this function. There are usually approx. 200–300 light-harvesting pigment molecules serving one PSII RC.

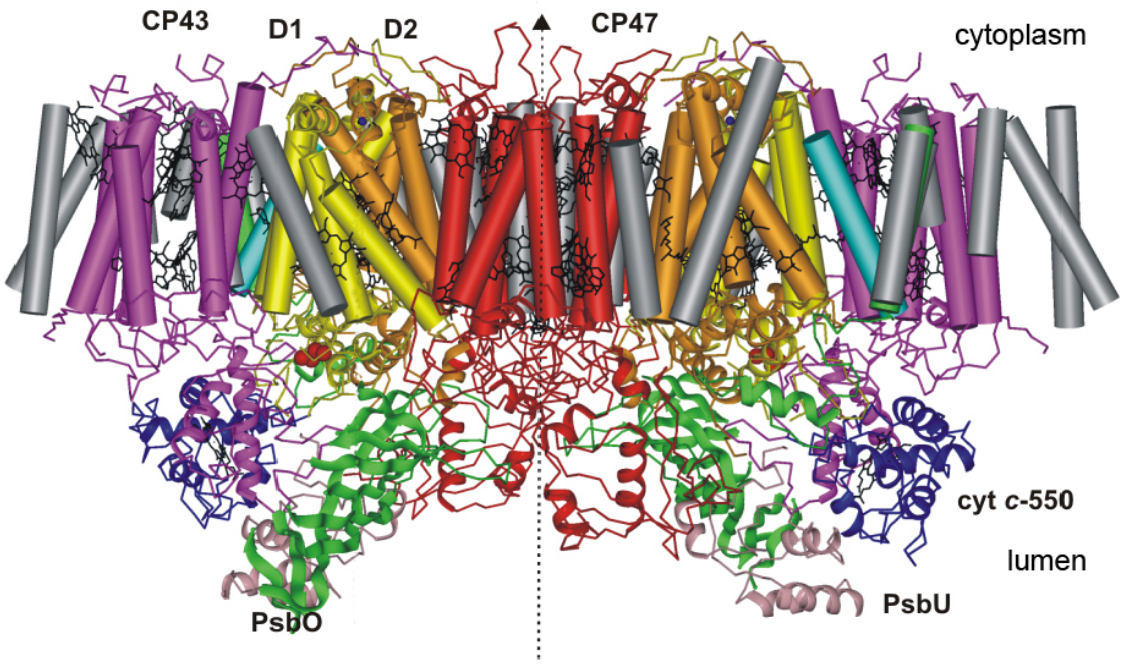

Figure 4 Structure of photosystem II from *Thermosynechococcus elongatus* at 3.0 Å resolution (Loll et al., 2005). The structure shows a PSII dimer with the color coded proteins: D1, yellow; D2, orange; CP47, red; CP43 magenta; α and ß-chain of Cyt b559, green and cyan; low molecular weight subunits, grey. The extrinsic proteins are labeled as follows: PsbO, green; PsbU (12 kDa extrinsic protein), pink; PsbV (Cyt c-550), blue.

The D1 and D2 proteins contain the cofactors that are involved in charge separation, leading to the oxidation of water and reduction of the terminal electron/proton acceptor, plastoquinone. Together, they bind six Chl*a* molecules, two Pheo (pheophytin) molecules, two PQs (plastoquinones), at least one β-carotene on the D2 side of the RC and a non-haem iron. An additional β-carotene on the D1 side has recently been assigned (Loll et al., 2005). The crystal structure at 3.0 Å resolution clearly shows (Figure 5) that these cofactors are also arranged around the local pseudo-C2 axis, which relates the transmembrane α-helices of D1 and D2, CP43 and CP47 (Zouni et al., 2000; Kamiya and Shen, 2003; Loll et al., 2005). The axis passes through the non-haem iron and through the middle of a cluster of four Chl*a* molecules called P_{D1}, P_{D2}, Chl_{D1} and Chl_{D2}, where the suffix denotes binding to the D1 or D2 protein. Similarly, the two pheophytins are referred to as $Pheo_{D1}$ and $Pheo_{D2}$. The PQs are positioned equally on each side of the non-haem iron and are bound to the Q_A and Q_B sites located within the D2 and D1 proteins, respectively.

The OEC is comprised of four Mn atoms as well as one atom of Ca^{2+}. It is unclear whether Cl^- is part of the OEC. At the OEC, the oxidation of water to molecular oxygen is catalyzed (Babcock et al., 1989; Debus, 1992; Tang et al., 1996).

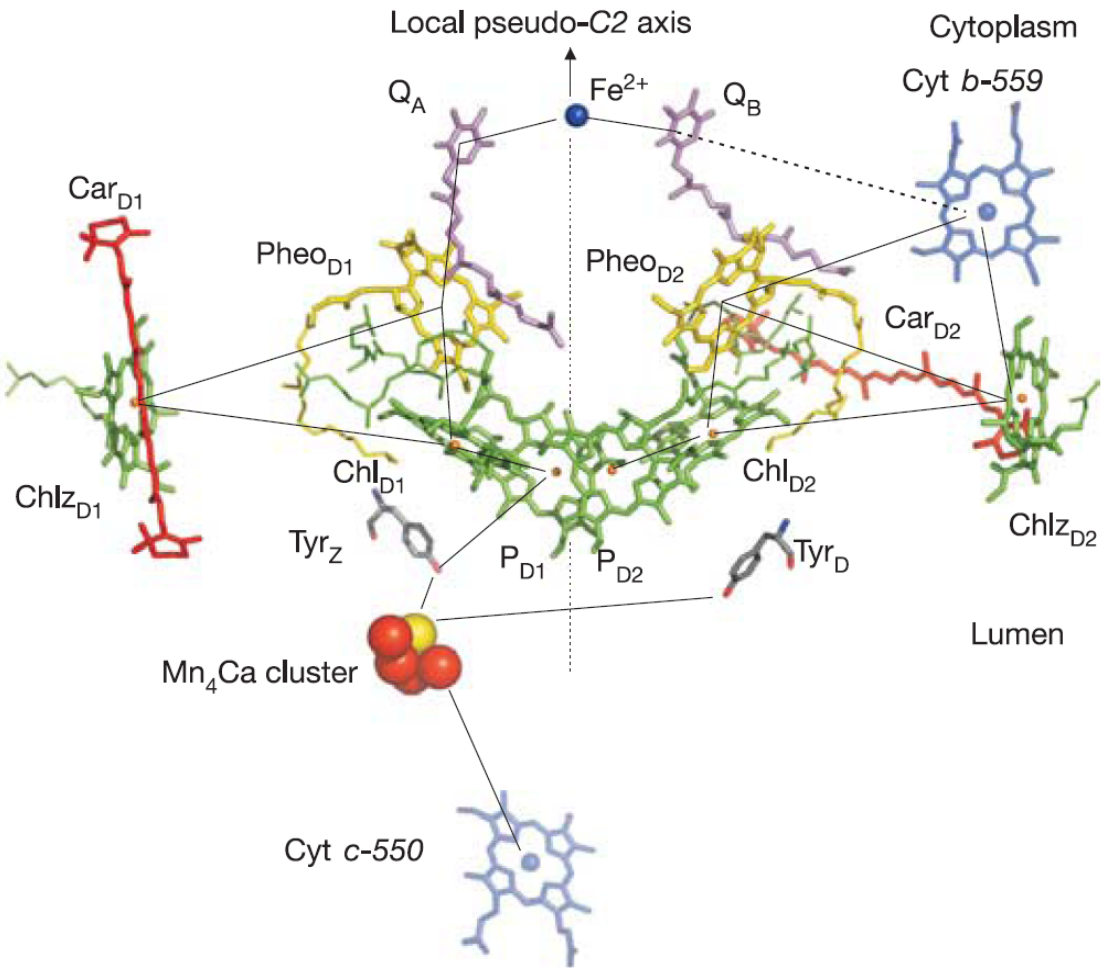

Figure 5 Arrangement of the cofactors involved in electron transport in PSII from Thermosynochocystis elongatus (Loll et al., 2005). The cofactors of the electron transfer chain (P_{D1}/P_{D2}, Chl_{D1}/Chl_{D2}, $Pheo_{D1}/Pheo_{D2}$, Q_A/Q_B) are related by the pseudo-C2 axis (arrow). Fe^{2+} (blue), Mn (red) and Ca^{2+} (yellow) ions are shown as spheres.

The role of Mn is to store the energy derived from the absorption of photons and use it to drive the thermodynamically unfavourable reaction of water oxidation. While Ca^{2+} has been found to be absolutely essential for catalytic activity, the role of Cl^- is unclear and their exact roles remain unknown. Both ions can be functionally replaced by other ions; Ca^{2+} can be replaced by Sr^{2+}, accompanied by a lower rate of oxygen evolution, and Cl^- can be replaced by Br^- with little effect on the rate of oxygen evolution, or by NO_2^-, NO_3^- and I^-, anions, which produce much lower activities (Kelley and Izawa, 1978; Ghanotakis et al., 1984; Sandusky and Yocum, 1984; Ghanotakis and Yocum, 1986; Ono et al., 1987; Homann, 1988). Recent crystallographic results on PSII from cyanobacteria clearly revealed the presence of a single Ca ion at a distance of about 3.0 Å from the Mn-complex (Ferreira et al., 2004). However, there were no indications for any halides in the vicinity of the Mn/Ca ions. On the other hand, XAS data at the Br K-edge from Cl^- depleted and Br^- –reconstituted containing and PSII from plant apparently revealed evidence for Cl–binding at ~5.0 Å to Mn (Haumann et al., 2006).

1.2.2 The Extrinsic Proteins

A great deal of structural information about the extrinsic proteins isolated from higher plants and cyanobacteria has been gathered in the last decades from various biophysical approaches (see review (Bricker and Burnap, 2005; Roose et al., 2007)).

The water soluble extrinsic proteins are peripherally bound to the lumenal side of PSII and are believed to maintain the stability and activity of the catalytic site (Chen et al., 1995; Seidler, 1996). In higher plants, the 33, 23- and 18-kDa extrinsic proteins are named according to their apparent molecular weight in SDS-gel electrophoresis. The 33 kDa protein is commonly found in higher plants and cyanobacterial PSII, and its function has been studied extensively. These studies indicate that the PsbO protein of plants and green algae has a very similar structure to that of cyanobacterial PsbO. Additionally, it stabilizes the Mn_4Ca-cluster in the dark and promotes the efficient redox cycling in the light (Vander Meulen et al., 2004).

In higher plants, the 23kDa (PsbP) and the 18 kDa (PsbQ) extrinsic proteins are bound to the lumenal side of PSII (De Las Rivas et al., 2004). In red algae and cyanobacteria, the 23 kDa and 18 kDa protein are absent and substituted by a 12 kDa (PsbU) protein and Cyt c550 (PsbV) (Shen et al., 1993; Hasler et al., 1997).

The 23- and 18-kDa extrinsic proteins appear to be required for optimal rates of O_2 evolution at physiological calcium and chloride concentrations (Seidler, 1996; Bricker and Frankel, 1998; Popelkova et al., 2004; Bricker and Burnap, 2005; Roose et al., 2007). Our current knowledge in relation to the structural information is still limited. Recently crystal structure of the 18 kDa protein was reported at 1.95 Å resolution (Calderone et al., 2003). If the 23kDa protein, diffraction data to a resolution of 2.0 Å were obtained (Ifuku et al., 2003).

In the absence of the PsbU and PsbV proteins, the rate of O_2-evolution was found to be strongly dependent on both Ca^{2+} and Cl^-, suggesting that these proteins perform a similar function to the 18- and 23-kDa extrinsic subunits in higher plants (Enami et al., 1998). A schematic drawing of PSII in spinach showing the extrinsic proteins is depicted in Figure 6(A). A view of the lumenal surface showing the extrinsic proteins PsbO, PsbU and PsbV at 3.0 Å resolution from *T. elogantus* is depicted in Figure 6 (B).

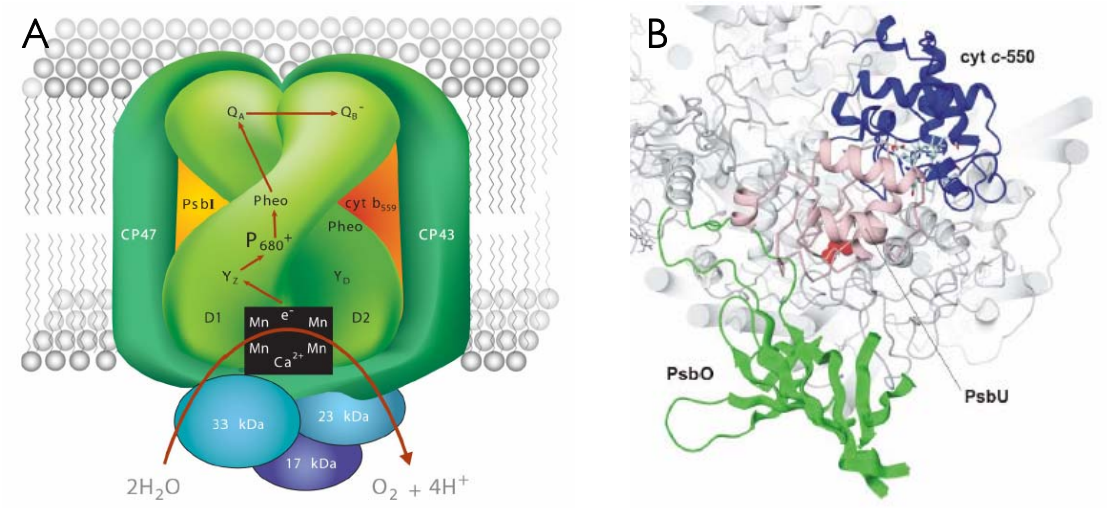

Figure 6 (A) Diagram of a core complex from spinach. The three extrinsic proteins are shown in blue and violet (Nelson and Ben-Shem, 2004). (B) View from the lumenal side of the membrane-extrinsic subunits (T. elogantus). Cyt c-550 in blue, PsbU in pink, PsbO (33 kDa) in green and all other subunits and cofactors are shown in grey (Loll et al., 2005)

1.2.3 Structure of the Mn cluster and mechanism of water oxidation and O_2 evolution

The catalytic cycle first formulated by Kok (Kok et al., 1970) establishes the starting point of our current understanding of photosynthetic water oxidation as well as the foundation for further studies on the chemical nature of the reaction intermediates. In 1969, Pierre Joliot and co-workers used dark-adapted algae and chloroplast to measure the release of oxygen during successive short (10µs) saturating flashes (Joliot et al., 1969). They discovered a characteristic periodicity of four in the oxygen yield, and by these measurements they demonstrated that four photochemical reactions are required for the release of one molecule of O_2. Figure 7 (A) shows a typical oxygen oscillation pattern of dark-adapted thylakoids. The main aspects of such patterns are: 1) a pronounced first maximum after the 3rd flash and further maxima after successive four flash intervals; 2) the damping of the O_2 release pattern.

In 1970, based on these experiments, Kok and coworkers developed a model for water oxidation by PSII (Kok et al., 1970). They proposed that in the dark-adapted algae, the water oxidizing complex (WOC) may exist in five states (S_0–S_4). Each state advances to the next upon an individual photochemical reaction (removing of one electron), resulting in the accumulation of four oxidizing equivalents in the WOC (yellow panel in Figure 7 (B)). Kok and coworkers proposed the miss (**α**) and double hit (**ß**) probabilities in order to explain the damping in the O_2 oscillation pattern (Kok et al., 1970).

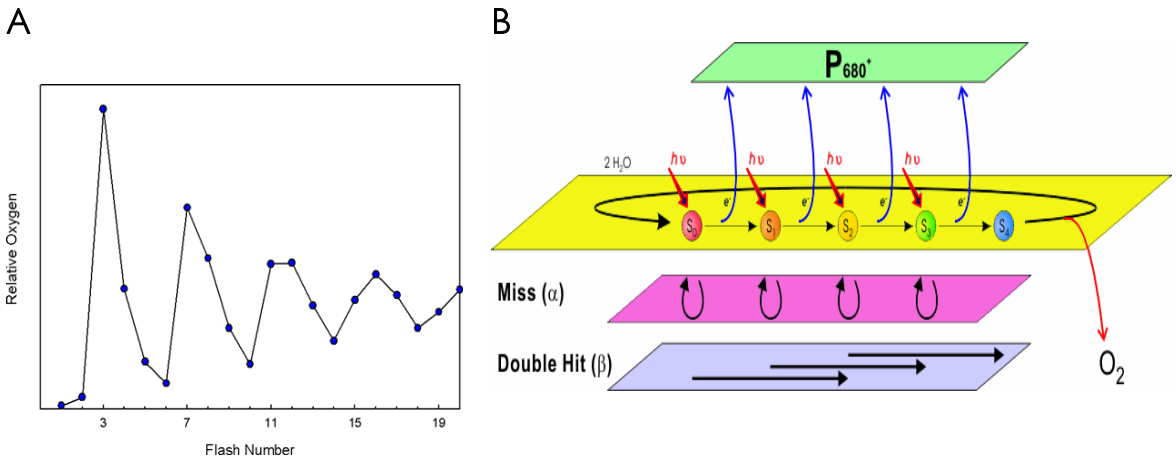

Figure 7 (A) Oxygen yield as a function of flash number showing the periodicity of four and the first maximum at the 3rd flash (Joliot and Kok, 1975). (B) Kok's cycle representation. Reprinted from http://www.rsbs.anu.edu.au/O2/O2_3_Photosystemll.htm.

The net reaction results in the release of one molecule of oxygen and four protons into the lumen and the sequential transfer of four electrons through the reaction center to the plastoquinone (Q_B). The states S_0, S_2 and S_3 are meta-stable and decay toward S_1 with half-times that strongly depend on temperature and pH (Vass and Styring, 1991; Messinger et al., 1993). While the S_2 and S_3 states decay in the second and minutes regime towards the S_1-state, the S_0 state require tens of minutes (Hillier and Messinger, 2005). All of the S-state transitions, apart from $S_4 \rightarrow S_0$, are induced by the photochemical oxidation of $P680^+$ which in turn oxidizes the OEC via a redox-active tyrosine. The $S_4 \rightarrow S_0$ transition is spontaneous and light-independent. Recent studies have revealed several intermediates in the overall $S_3 \rightarrow S_4 \rightarrow S_0$ transition. Our group has shown by time–resolved x-ray spectroscopy that in the $S_3 \rightarrow S_0$ transition a distinct and kinetically resolvable intermediate is formed within about 200 µs prior to the onset of O-O bond formation (Haumann et al., 2005a). This intermediate is specifically found in the x-ray transients for the $S_3 \rightarrow S_0$ transition induced by the 3rd laser flash (Dau and Haumann, 2007b) (Figure 8).

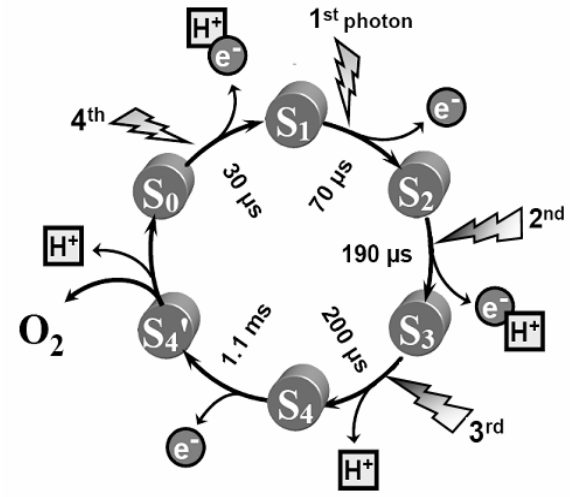

Figure 8 Extended S-state cycle of water oxidation (Haumann et al., 2005a) and relation of electron and proton removal in the individual S-state transitions. A complete cycle requires sequential absorption of four photons, which can be provided in form of four ns-Laser flashes. Each flash results in formation of $Y_Z^{\bullet+}$ within less than 1 µs; the subsequent processes at the PSII donor side are summarized in the shown above. Dark adaptation results in formation of the S_1-state in the majority of PSII so that the first flash induces the $S_1 \rightarrow S_2$ transition. For each transition it is indicated whether an electron is transferred from the Mn complex to the oxidized Y_Z, whether a proton is released from the Mn complex or its ligand environment, and whether or not the rate constant is sensitive to pH and H_2O/D_2O exchange.

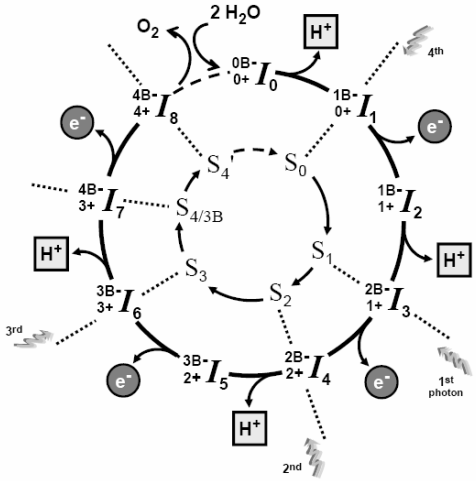

Figure 9 Proposed sequence of alternating proton and electron abstraction from the Mn complex. Electrons and protons are removed from a Mn complex that includes the Mn_4Ca-µ-oxo core and its ligand environment, but not the tyrosine denoted as Y_Z. The indicated electron removal (i.e., oxidation of the Mn complex) proceeds by electron transfer to the Y_Z-radical, which is formed within less than 1 µs after absorption of a photon. Not the light-induced $Y_Z^{\bullet+}$ formation, but only the subsequent processes of Mn-complex oxidation or proton release from the Mn complex are indicated in the scheme.

Experimental findings on the properties of the individual S-state transitions are summarized in Table 1, which has been adapted from (Dau and Haumann, 2007a). Recently, Dau and co-workers have presented a model of alternating proton and electron removal (Figure 9). Protons and electrons are removed strictly alternately from the Mn complex. Nine states are associated with the reaction cycle, starting with I_0, eight successive steps of alternate protons and electron removal lead to I_8 and only then the O-O bond is formed. Therefore, four oxidizing equivalents as well as four deprotonated groups are accumulated prior to the onset of O_2-evolution (Figure 8a). The authors emphasize that the I-states exclusively denote states of the Mn complex (Dau and Haumann, 2007a).

Table 1 Experimental findings on the properties of the individual S-state transitions. (+) Presence, (-) Absence. Sources: a) (Renger, 1992; Kretschmann and Witt, 1993; Kretschmann et al., 1996; Haumann et al., 1997; Schlodder and Witt, 1999); (b) (Fowler, 1977; Saphon and Crofts, 1977; Bowes and Crofts, 1978; Dismukes and Siderer, 1981; Wille and Lavergne, 1982; Förster and Junge, 1985; Haumann et al., 1994; Kretschmann et al., 1996; Haumann et al., 1997; Schlodder and Witt, 1999; Dau et al., 2003) ; (c) (Witt and Zickler, 1974; Beck et al., 1985; Miller and Brudvig, 1989; Renger, 1992; Lavergne and Junge, 1993; Haumann et al., 1997; Schlodder and Witt, 1999; Junge et al., 2002; Haumann et al., 2005a; Dau and Haumann, 2007b); (d) (Haumann and Junge, 1994; Rappaport et al., 1994; Haumann et al., 1997; Razeghifard and Pace, 1999; Robblee et al., 2001; Junge et al., 2002; Grabolle, 2005a; Haumann et al., 2005a; Haumann et al., 2005b; Dau and Haumann, 2006; Dau and Haumann, 2007b).

Transition	electron transfer Mn_4Ca complex → Y_Z	proton removal	pHdependence	halfstime [µs]	K_D/K_H ratio
$S_0 \rightarrow S_1$ (a)	+ (I_1–I_2)	+ (I_2–I_3)	–	30	< 1.1
$S_1 \rightarrow S_2$ (b)	+ (I_3–I_4)	–	–	70	≤ 1.3
$S_2 \rightarrow S_3$ (c)	+ (I_4–I_5)	+ (I_5–I_6)	+	190	1.4 – 2.0
$S_3 \rightarrow S_0$ (d)	+	++	+	1200	
$S_3 \rightarrow S_4$	–	+ (I_6–I_7)		200	
$S_4 \rightarrow S_{4'}$	+ (I_7–I_8)	–	–	1100	1.2 – 1.4
$S_{4'} \rightarrow S_0$	–	+ (I_8–I_0)			

1.2.4 Atomic structure of the Mn_4 Cluster

A number of structural models of the OEC (Debus, 1992; Messinger et al., 1995; Britt, 1996; Diner and Babcock, 1996; Witt, 1996; Yachandra et al., 1996; Lundberg and Siegbahn, 2004; Messinger, 2004) and mechanistic schemes (Pecoraro et al., 1998; Robblee et al., 2001; Vrettos et al., 2001; Barber et al., 2004; Britt et al., 2004; McEvoy and Brudvig, 2004; Messinger, 2004; McEvoy et al., 2005a; McEvoy et al., 2005b) have been proposed in attempts to elucidate the catalytic cycle at the detailed molecular level. However, many fundamental aspects of the proposed mechanisms and structure intermediates are the subject of current debate (Messinger, 2004; McEvoy et al., 2005a; McEvoy et al., 2005b). Many of the designed mechanisms depend critically on the structure of the Mn_4Ca complex. In fact, as long as the structure of the Mn_4Ca complex is not resolved at the atomic level, it may not be possible to establish unequivocal functional models of the OEC S-states.

X-ray absorption spectroscopy (XAS) (Dau et al., 2001; Robblee et al., 2001; Dau and Haumann, 2003; Dau et al., 2003) and electron paramagnetic resonance (EPR) (Dismukes

and Siderer, 1981; Messinger et al., 1997; Britt et al., 2000) studies have revealed structural details of the OEC as outlined below.

1.2.5 Oxidation states of manganese

X-ray absorption, emission spectroscopy of Mn, and EPR have been used to investigate the oxidation state of the Mn complex in its catalytic cycle.

The results of the studies can be summarized as follows:

There is consensus that at least three of the S-state transitions involve manganese oxidation. Investigating the oxidation states of Mn for the S_0, S_1, S_2 and S_3 by means of XANES (Roelofs et al., 1996) proposed that Mn is oxidized during the $S_0 \rightarrow S_1$ and $S_1 \rightarrow S_2$ transitions, but is not oxidized during the $S_2 \rightarrow S_3$ transition. Both (Ono et al., 1992) and (Iuzzolino et al., 1998), contrary to the interpretation mentioned above, have suggested that Mn is oxidized during each S-state transition. Until today, the controversy is not settled. Using the so-called integral method (Dau et al., 2003) to determine the Mn K-edge energy of the four S-states (measured at 20 K and, for the first time, at room temperature), our group has found a significant shift of the K-edge position to higher energies, on all three oxidizing transitions (Table 2). The magnitude of each of these shifts (~0.7 eV) is compatible with oxidation of one Mn ion. As demonstrated elsewhere (Dau and Haumann, 2003; Dau et al., 2004), we have found that the changes in edge shape and position observed for the $S_2 \rightarrow S_3$ step are straightforwardly explained by a transition from five coordinated Mn^{III} to six-coordinated Mn^{IV}. The transformation of $Mn^{III}L_5$ to $Mn^{IV}L_6$ is supported by EXAFS data, indicating that in contrast to the other oxidizing S-state transitions, the average Mn-ligand bond length is not shortened on $S_2 \rightarrow S_3$. Furthermore, the formation of an additional μ-oxo bridge on $S_2 \rightarrow S_3$, suggested by the EXAFS results, provides a straightforward rationale to explain the coordination number change.

Table 2 Changes in the K-Edge energies of the Mn complex upon S-state transitions[(a)]

	K-Edge energy of the S_1-state (eV ± 0.1)	Difference in K-edge energies of the S-states[(b)] (eV)			
data set	E_1	$E_1 - E_0$	$E_2 - E_1$	$E_3 - E_2$	$E_0 - E_3$
20 K	6551.62	0.58	0.76	0.71	-2.05
RT	6551.79	0.57	0.79	0.70	-2.06

[(a)] The values correspond to spectra measured at 20 K and RT by the sampling -XAS technique.
[(b)] K-Edge energies were derived by the "Integral method" (Dau et al., 2003).

1.2.6 Structural changes in the S-state transitions

Indications for structural changes in the μ-oxo core of the Mn_4Ca complex in the S-state cycle have been obtained by XAS (Figure 10) (Dau et al., 2001; Robblee et al., 2001; Dau and Haumann, 2003). In the S_0-state, EXAFS analysis suggests the presence of two Mn-Mn vectors with distinctly different length: one close to 2.7 Å (~2.72 Å) and the second one slightly longer than 2.8 Å (~2.84 Å). These distances have been tentatively attributed to a Mn-(μ-O)$_2$-Mn unit (2.7 Å), and to a Mn-(μ-OH)(μ-O)-Mn motif (2.8 Å).

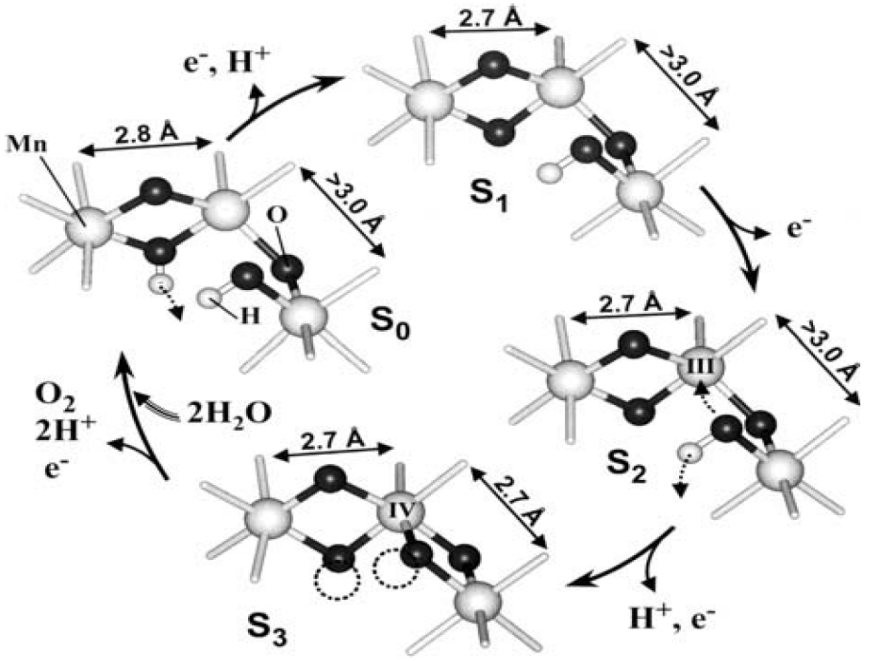

Figure 10 Scheme of structural changes of the Mn complex in the water-oxidation cycle (from (Haumann et al., 2005b)). For clarity, only three Mn ions of the Mn_4Ca-complex are shown which suffices to illustrate the putative modifications in the structure of the complex. The omitted fourth Mn is assumed to be connected to one of the depicted Mn ions by a di-μ-oxo bridge leading to a further Mn–Mn vector of ~2.7 Å (in all S-states). One Ca ion (not shown) presumably is connected by two or more bridging oxygens (μ-O, μ-OH, μ-OH_2) to two or more Mn ions. Alternatively to the depicted Mn-(μ$_2$-O)$_2$-Mn-(μ$_2$-O)-Mn motif in the S_1-complex, a Mn_3(μ$_2$-O)(μ$_3$-O) motif might be present which then is transformed to a Mn_3(μ$_2$-O)$_2$(μ$_3$-O) unit in the S_2 → S_3 transition. Single-electron oxidation of manganese is assumed to occur on S_0 → S_1, S_1 → S_2, and S_2 → S_3, but only the oxidation state of the five-coordinated Mn(III) (in S_2) which is transformed into a six-coordinated Mn(IV) (in S_3) is indicated by roman letters inside of the respective Mn-sphere. Ligand deprotonation and rearrangement presumably taking place in the subsequent S-state transition are emphasized using dotted arrows. In S_3, dotted circles mark the sites where bridging oxides may act as proton acceptors in S_3→S_0, the oxygen-evolution transition (Haumann et al., 2005b).

In the S_1-state, the two Mn-Mn vectors of ~2.72 Å length are of only slightly different length, presumably close to 2.69 and 2.74 Å, pointing towards the presence of two Mn-(μ$_2$-O)$_2$(μ$_{2/3}$-O)-Mn units (Dau et al., 2004). The shortening of the ~2.84 Å Mn-Mn distance present in S_0 to a 2.72 Å distance in S_1 is straightforwardly explained by oxidation and deprotonation of a $Mn^{II}Mn^{III}$(μ-O)(μ-OH) unit present in S_0 to yield a $Mn^{III}{}_2$(μ-O)$_2$ unit in S_1.

In conclusion, the $S_0 \rightarrow S_1$ transition likely involves a change in the Mn-Mn bridging mode, possibly the deprotonation of a singly protonated di-μ-oxo bridge leading to two Mn-$(\mu\text{-O})_2$-Mn units (or motifs) in the S_1-state.

In relation to the $S_1 \rightarrow S_2$ transition, the EXAFS data on $S_2 \rightarrow S_3$ excludes changes in the Mn – Mn bridging mode of the two di-μ-oxo bridge units, but does not allow for any conclusion with respect to the deprotonation of a terminal ligand. Electrochromic data suggests that a positive charge is acquired by the Mn complex in the $S_1 \rightarrow S_2$ transition (Haumann and Junge, 1996; Junge et al., 2002), a finding difficult to reconcile with Mn oxidation coupled to ligand deprotonation. In summary, this transition involves a Mn(III)→Mn(IV)oxidation which likely is neither coupled to any changes in the Mn-Mn bridging mode nor to any ligand deprotonation. In the $S_2 \rightarrow S_3$ transition, the observed increased in the number of 2.7 Å vectors from two, in the S_2-state, to three, in the S_3-state, suggests an increase in the number of di-μ-oxo bridged Mn-Mn motifs. The formation of a third di-μ-oxo bridge likely involves a change from mono-μ-oxo bridging to di-μ-oxo bridging by formation of an additional μ-oxo bridge. We propose that the μ-oxo bridge formation involves the transformation of five-coordinated Mn(III)to six-coodinated Mn(IV).

A summary (Table 3) for all four S-states is presented in order to point out the most recent and relevant information on the S-states.

Table 3 Overview of the recent assignments for S-states in Mn_4Ca, showing the methods used, alternative assignations and corresponding references.

S-state	assignment	methods	reference
S_0	Mn_4 (II, III, IV_2)	[1] XANES [2] XAS [3] XES	[1] (Haumann et al., 2005b) [2] (Guiles et al., 1990; Riggs et al., 1992; Iuzzolino et al., 1998) [3] (Messinger et al., 2001)
	Mn_4 (III_3, IV)	[1] XANES [4] ^{55}MnENDOR	[1] (Haumann et al., 2005b) [4] (Kulik et al., 2005)
S_1	Mn_4 (III_2,IV_2)	[1] XANES [2] EXAFS [3] XES [4] UV/vis	[1] (Yachandra et al., 1987; Roelofs et al., 1996; Haumann et al., 2005b) [2] (Cole et al., 1987) [3] (Bergmann et al., 1998; Messinger et al., 2001) [4] (Dekker et al., 1984)
	Mn_4 (III_4)	[1] EPR	[1] (Zheng and Dismukes, 1996; Kuzek and Pace, 2001)
S_2	Mn_4 (III, IV_3)	[1] XANES [2] XAS [3] XES [4] ^{55}Mn ENDOR [5] EPR [6] SCR	[1] (Iuzzolino et al., 1998; Haumann et al., 2005b) [2] (Roelofs et al., 1996; Yachandra, 2005) [3] (Messinger et al., 2001) [4] (Peloquin and Britt, 2001) [5] (Hasegawa et al., 1998; Hasegawa and Ono, 1999)
	Mn_4 (III_3,IV)	[1] EPR	[1] (Zheng and Dismukes, 1996)
S_3	Mn_4 (III, IV_3)	[1] XANES [2] XAS [3] XES [4] ^{55}Mn ENDOR	[2] (Roelofs et al., 1996; Yachandra, 2005) [3] (Messinger et al., 2001)
	Mn_4 (IV_4)	[1] XANES	[1] (Pecoraro and Hsieh, 2000; Haumann et al., 2005b)

1.2.7 Advances in crystallographic studies

During the last five years a major breakthrough in the elucidation of the photosynthetic water oxidation has been achieved by crystallographic studies (Zouni et al., 2001; Kamiya and Shen, 2003; Biesiadka et al., 2004; Ferreira et al., 2004; Loll et al., 2005). These structures, while currently limited to a resolution of 3.0 Å, have located the electron density associated with the Mn and Ca in the multi-protein PS II complex and unambiguously resolved most of the amino acid residues in the protein and nearly all cofactors (Satoh et al., 2005).

The 3.8 Å resolution structure (*T. elogantus*) (Zouni et al., 2001) provided information on the arrangement of cofactors involved in exciting energy transfer and charge separation. The model confirmed the dimeric organisation of the isolated complex and the relative positioning of the major subunits and their transmembrane helices within each monomer previously derived from electron crystallography (Barber, 2002). However, the essential cofactors Ca^{2+} and Cl^- were not located in this structure. The Mn_4 cluster was shown to be coordinated predominantly by amino acid residues of the D1 subunit of PSII. Three Mn atoms were positioned roughly at the three corners of a triangle, and the fourth Mn was placed at the center of the triangle (Zouni et al., 2001).

Subsequently, in the 3.7 Å resolution crystal structure (*T. vulcanus*) (Kamiya and Shen, 2003), the shape of the Mn_4 unit was shown to be very similar to that of the previously reported structure (3.8 Å). The data provided additional information with respect to the coordination environment of the Mn atoms. At least four to five bonding interactions between the Mn cluster and the D1 polypeptide were established. Several other residues were also identified as possible ligation sites for the Mn cluster (Figure 11 A). However, neither Ca^{2+} nor Cl^- ions were located in this structure.

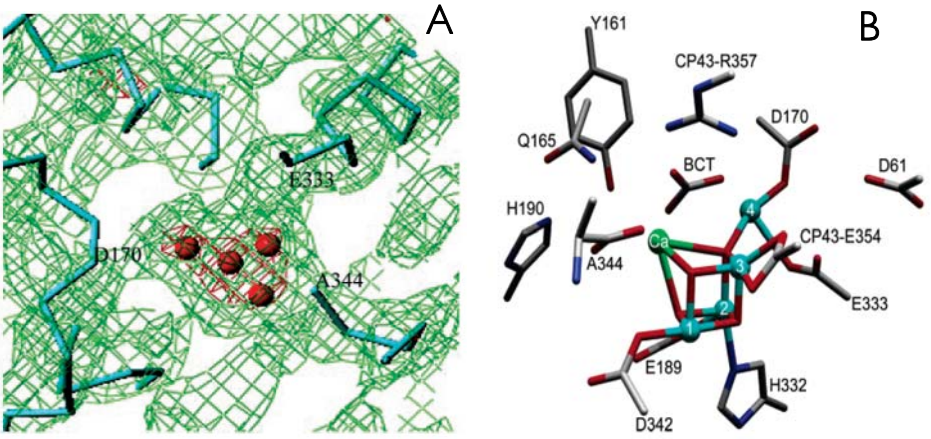

Figure 11 (A) Spatial arrangements of the PSII Mn_4 cluster in *T. Vulcanus* as shown in the crystal structures at 3.7 Å. (B) Organization of the Mn_4Ca cluster and their possible ligands, reported by Ferreira et al. The Mn ions are shown in cyan, calcium is in green, oxygen is in red, carbon is in gray, and nitrogen is in blue. BCT denotes bicarbonate, which was modelled in the x-ray structure. Unless otherwise indicated, amino acid residues belong to the D1 subunit.

A crystal structure from *T. elongatus* at 3.5 Å, resolved by Ferreira et al. (Ferreira et al., 2004) was an important progress, as it provided a first glimpse of the structural organization of the Mn complex itself. The improved quality of the electron density map in the 3.5 Å structure allowed to assign almost all of the amino acids to the Mn_4Ca cluster (Barber, 2006). In addition, the catalytic center was shown to contain one Ca^{2+} ion (Figure 11 B). There was non-protein electron density in the vicinity of Mn4 and Ca^{2+}, which was tentatively assigned to a bicarbonate ion (BCT) (Figure 11B).

A subsequent study of *T. elongatus* at improved resolution of 3.0 Å revealed the locations and interactions between 20 protein subunits and 77 cofactors per monomer, and provided so far the highest level of refinement of the PSII structure. The structure of the metal cluster is consistent with information derived from EXAFS measurements. The assignement of amino acids residues coordinating the manganese cluster was refined. Head groups and side chains of the organic cofactors (carotenoids, lipids, Chls) were modelled, coordinating amino acids identified and the nature of the binding pockets of the quinines derived. Coordinating amino acids of the manganese cluster, where oxidation of water to oxygen is catalysed and of redox-active Tyr_Z and non-haem Fe^{2+} were determined.

It is worth noting that the interatomic distances within the Mn_4–Ca cluster could not be resolved directly in the electron density map at 3.0 Å resolution (Kern et al., 2007). Loll et al. suggested an OEC structure, which contains four Mn cations, arranged in an "L" shape (Figure 12). The distance between the Mn1 and Mn2 atoms, as well as the Mn2 and Mn3 atoms, was 2.7 Å, indicating di-μ-oxo bridges, while the Mn1-Mn3 and Mn3-Mn4 distances was 3.3 Å long, representing mono-μ-oxo bridges. The crystal structure at 3.0 Å resolution, shows the Ca^{2+} ion in a trigonal pyramidal arrangement in a position equidistant from three Mn atoms (about 3.4 Å) and at 5 Å distance to the hydroxyl group of tyr_Z (Figure 12). This small distances between Ca^{2+} and tyr_Z, has been interpreted as suggesting an essential role of Ca^{2+} for effective functioning of water oxidation (Kern et al., 2007).

On the basis of polarized x-ray absorption spectroscopy study on oriented single crystals of PSII from cyanobacteria, using an x-ray dose below the threshold of damage, possible structures for the Mn_4Ca cluster and the orientation of the cluster in the PS II crystal (Figure 13) were modelled (Yano et al., 2006).

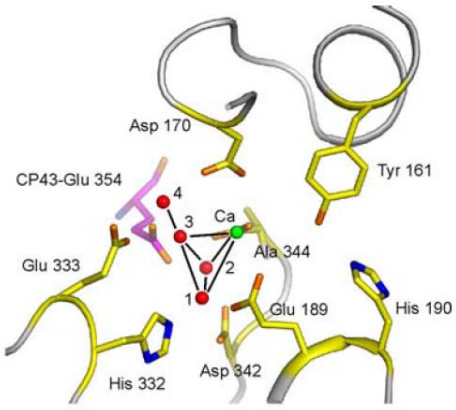

Figure 12 Model of the Mn_4Ca cluster derived from the X-ray crystal structure at 3.0 Å resolution. View along the membrane plane with the lumenal side on the bottom. The spheres represent Mn cations (red) as well as the Ca^{2+} (green) (Loll et al., 2005).

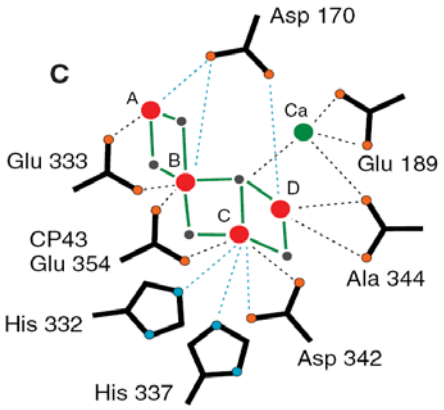

Figure 13 Schematic view of one of the four EXAFS derived models of the Mn_4Ca cluster with putative ligands. The spheres represent Mn (red), Ca (green) and the bridging oxygen ligand atoms (gray). The assignment of ligands is tentative because it is based on the electron density of the Mn_4Ca cluster, and its immediate environment which may be altered by x-ray damage (Yano et al., 2006).

Our group recently presented a tentative model of the Mn complex in its S_1-state (Figure 14). The μ-oxo bridging between metal ions was chosen such that the final model i) matched the EXAFS results obtained on isotropic and uni-directionally oriented PSII samples and ii) could account in a straightforward way for structural changes in the S-state cycle.

Starting with the coordinates of (Loll et al., 2005), minimization of the potential energy was carried out by allowing for changes in the coordinates of atoms within a narrow range around Mn1, Mn2, and Mn3, but within a clearly extended range around Mn4, to account for the putative influence of radiation-induced modifications on Mn4 and its ligand environment. In the shown model, Mn1 and Mn2 are close to the original coordinates of (Loll et al., 2005); Mn3 is moderately shifted, but the positions of Mn4 and the Asp^{170} deviate clearly from the initial model (Loll et al., 2005). The $S_0 \rightarrow S_1$ transition is supposed to involve deprotonation of the μ_2-oxo bridge between Mn3 and Mn4. Up to the S_2-state, the hydroxide bridging between Mn2 and Ca is only loosely ligated to Mn1 (Mn1–O distance > 2.5 Å). In the $S_2 \rightarrow S_3$ transition, the five-coordinated Mn1 is oxidized and transformed into a six-coordinated Mn(IV), a process associated with deprotonation and proton release. In the thereby formed S_3-state complex, a $Mn_3Ca(\mu\text{-}O)_4$ cubane is present. The model implies that the substrate-water molecules bind at or close Mn4 because (i) only Mn4 is coordinatively not fully saturated by μ-oxo and amino-acid ligands and (ii) there is sufficient space around Mn4 to account for several water molecules. For further details, see (Dau et al., 2007)

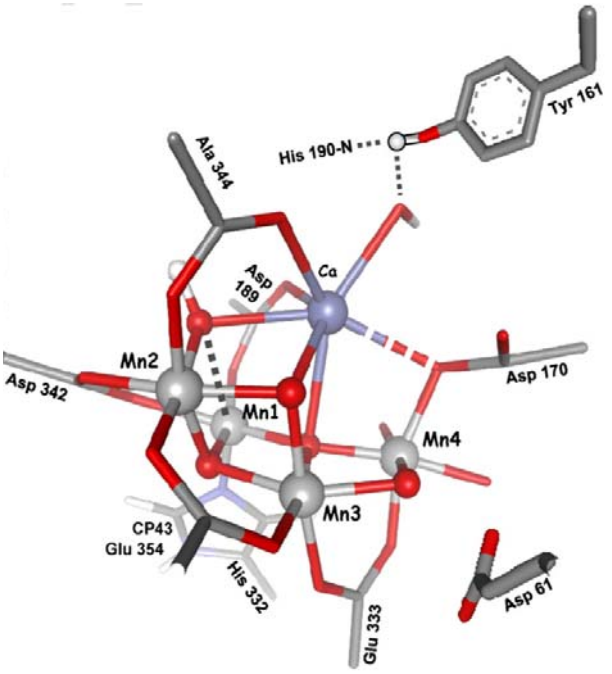

Figure 14 Tentative model of the Mn complex in its S_1-state. The ligands are assigned according to the crystallographic model at 3.0 Å (Loll et al., 2005). Molecular mechanics modeling was employed where a standard force-field had been complemented by reasonable constraints for the Mn–ligand distances and Mn–Mn distances (Dau et al., 2007).

1.2.8 Identification of putative ligands to the Mn_4Ca cluster

Conclusive lines of evidence suggest that Mn and Ca^{2+} ions in PS II are coordinated primarily by residues located in the carboxy-terminal region of the D1 polypeptide (for reviews, see (Debus, 1992; Diner, 2001)). Site-directed mutations in the D1 polypeptide of PSII have involved histidine and carboxylate residues in the coordination and assembly of the Mn_4Ca cluster (Debus et al., 2001; Diner, 2001; Wydrzynski and Satoh, 2005).

On the basis of mutagenesis studies, possible ligands of the Mn_4Ca cluster were considered to include: D1-Glu^{333}, D1-Asp^{342}, D1-Asp^{170}, D1-His^{332}, D1-His^{337}, D1-Asp^{59}, D1-Asp^{61} and D1-Asp^{342}.

Both Asp^{170} and Glu^{333} of the D1 polypeptide were found to form part of the high affinity binding site for the first Mn^{2+} ion that is photooxidized during the photoactivation of the Mn complex (Debus et al., 2001; Burnap, 2004). Moreover, these ligands may influence the coordination and redox properties of the photooxidized Mn^{2+} (Campbell et al., 2000; Debus et al., 2003). The coordination of Mn4 by Asp^{170} and Glu^{333} in the 3.5 Å resolution model suggests that this could be the Mn bound to the high affinity binding site (Kern et al., 2007).

Although PSII mutated at positions His^{337} and His^{332} showed only low rates of O_2 evolution and was incapability to assemble the Mn_4Ca cluster, none of these His seems to be involved in binding of the first Mn^{2+} during photoactivation (Nixon and Diner, 1994). However, the 3.0 Å resolution model shows that Mn1 is ligated by D1-His^{332} and that the side chain of His^{337} is not in a position to provide direct ligation to a Mn (Figure 15) (Loll et al., 2005).

The 3.5 Å resolution structural model revealed Ala^{344} as a possible ligand of Ca^{2+} (Ferreira et al., 2004). However, more recent FTIR spectroscopy studies have shown that D1-Ala^{344} binds to a redox-active Mn ion rather than to Ca^{2+} (Strickler et al., 2005).

In the recent 3.0, 3.2 and 3.5 Å X-ray crystallographic structural models, D1-Glu^{333} was identified as a ligand of Mn4 (Figure 15), which is also ligated by Asp^{170} (Biesiadka et al., 2004; Ferreira et al., 2004; Loll et al., 2005). Whereas in the 3.5 Å model, both carboxylate residues are unidentate ligands to Mn (Ferreira et al., 2004), in the 3.0 Å model, both carboxylate residues are bidentate ligands, although D1-Asp^{170} binds strongly asymmetric (Biesiadka et al., 2004). Mutational and spectroscopic studies have revealed that Mn4 does not undergo oxidation during the S-state cycle and that it is most prone to radiation damage and subsequent disordering.

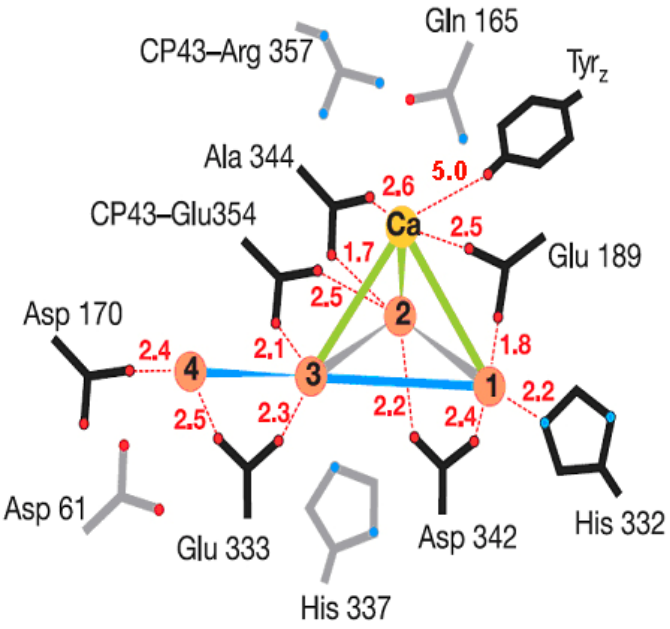

Figure 15 Schematic view of the Mn_4Ca cluster at 3.0 Å resolution. Distances between Mn (red) and Ca^{2+} (orange) are indicated by the connecting lines (grey, 2.7 Å; blue, 3.3 Å, green, 3.5 Å). Amino acids of the first coordination sphere are black; those of the second sphere are grey; distances are given in Å (Loll et al., 2005).

In contrast to previous findings (Ferreira et al., 2004), Glu^{189} and Ala^{344} in D1 are identified as possible ligands of Ca^{2+}, with the former also ligating Mn1 and the latter Mn2. Considering the position error of Ca^{2+} and results from FTIR spectroscopy indicating that Ala^{344} of D1 should ligate Mn (Kimura et al., 2005) but not Ca^{2+} (Strickler et al., 2005), apparently Ca^{2+} is coordinated only by the Glu^{189} of D1.

1.2.9 Radiation Damage of the Mn complex (X-ray photoreduction)

Currently, there is serious disagreement between the models of the Mn_4Ca complex in the published x-ray crystallography studies, and there are inconsistencies with X-ray absorption, EPR, and FTIR spectroscopic data (Yachandra et al., 1996; Peloquin et al., 2000; Cinco et al., 2004; Dau et al., 2004; Messinger, 2004; Debus et al., 2005; Kimura et al., 2005).

Radiation damage is an obstacle to the interpretations of the crystallographic results. XAS results on this process can be summarized as follows:

- The PSII crystals used in crystallographic assays suffer from radiation damage during x-ray data collection especially around the metal sites. By x-ray photoreduction, the higher valence states are reduced of Mn to Mn(II) (Yano et al., 2005; Kern et al., 2007).
- X-ray photoreduction of Mn is accompanied by changes in the metal coordination environment (even at 10 K), the Mn-Mn distances and overall geometry may change.
- Even at temperatures as low as 10 K, x-ray-induced photoreduction of the manganese complex is coupled to the loss of most or all μ-oxo-bridging motifs between manganese ions. Moreover, bridge disruption, may influence the positions of the putative Mn and Ca ligands (Debus et al., 2005; Grabolle et al., 2006; Kargul et al., 2007).
- The final Mn(II) state created at low temperatures spectroscopically resembles the $[Mn(II)(H_2O)_6]^{2+}$ complex in solution. A straightforward interpretation of this observation is that not only μ-oxo bonds are broken but that also rearrangements of the manganese ions and of their ligands from amino acids occur so that additional H_2O molecules may become bound directly to Mn(II) (Grabolle et al., 2006).

In order to obtain reliable structural models, future X-ray crystallographic studies will require an improvement in crystal quality and the adoption of procedures to elliminate the problem of radiation damage and at the same time to improve the spatial resolution.

1.3 Disassembly of the Mn complex of PSII by elevated temperatures.

Gradual disassembly of the Mn complex induced by biochemical treatments (Penner-Hahn, 1999) or exposure to a rapid temperature jump have been used to obtain information about the oxidation state and structural aspects of the intermediates involved in the catalytic cycle of water oxidation.

Considering that the donor side of PSII is more sensitive to heat than the acceptor side (Berry and Björkmann, 1980; Nash et al., 1985; Coleman et al., 1988) moderate heating can be used to initiate the stepwise disassembly of the tetramanganese complex (Pospisil et al., 2003).

In intact organisms and in *vitro* it is known that the thermodynamically favored state of Mn is Mn(II) (at pH 6.5). In PSII membrane particles it takes days to obtain a complete reduction of the high valency Mn ions (i.e. Mn(III) and Mn(IV)) to aqueous Mn(II), concomitantly with protein degradation(Ono, 2001).

In our group the intermediates of the thermally activated disassembly process have been studied and, it was found that the disintegration or disassembly process involves at least three kinetic phases and distinct intermediates. The trigger event is a rapid increase in temperature (temperature jump). Suitable protocols involve exposure of PSII multilayer membranes to a temperature jump (from 20°C to 47°C), followed by rapid cooling after heating times ranging from 0 to 180 min. This treatment allows the detailed analysis of the time course of the heat-induced changes at the Mn complex by oxygen polarography, delayed fluorescence, atomic absorption spectroscopy (AAS), polyacrylamide gel electrophoresis, EPR spectroscopy and x-ray absorption spectroscopy, which in part, has been performed in this thesis.

Previous results suggested that the first heat jump response involves rapid Ca release from the Mn complex, followed by the slower release of (2+2) Mn^{2+} ions (Pospisil et al., 2003).

The oxygen-evolution activity was measured in the presence of 55 mM of $CaCl_2$ (instead of 5 mM). Under these high-calcium conditions, the loss of oxygen evolution is retarded (Figure 16, open circles). The use of 50mM of $MgCl_2$ plus 5 mM of Ca^{2+}, however, does not retard the deactivation (Figure 16, triangles). This observation suggests that the heat-induced loss in oxygen-evolution activity is indeed closely related to the release of calcium (Pospisil et al., 2003). When Ca release was related to the extrinsic proteins was investigated in this thesis.

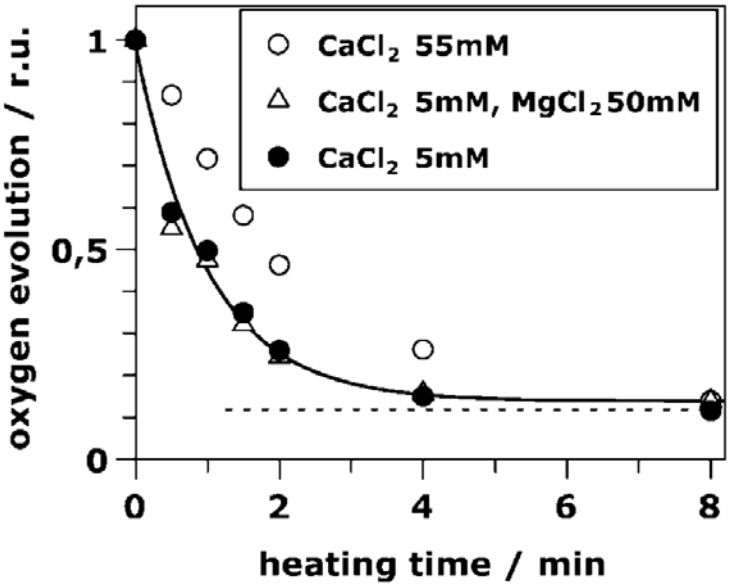

Figure 16 Relative oxygen-evolution activity of resuspended PSII samples previously exposed to 47°C for various time periods. Oxygen evolution was measured in the presence of 5 mM $CaCl_2$ (solid circles), 5 mM $CaCl_2$ plus 50 mM $MgCl_2$ (open triangles) and 55 mM $CaCl_2$ (open circles).

The heat-induced changes in the magnitude of two EPR signals were monitored. In PSII the Tyr-161 of the D2 protein, which is not actively involved in the PSII electron transfer chain, mostly is present as a radical, the Y_D^{ox} radical (Debus et al., 1988; Vermaas et al., 1988). Reduction of the Y_D^{ox} radical necessarily results in the disappearance of the associated EPR signal. The amplitude of the Y_D^{ox} signal rapidly decreased with heating time and was close to zero after ~2 min. After longer heating times only a small signal remained. The decrease of the Y_D^{ox} signal can be well described by a single exponential with the same rate constant as observed for the loss of oxygen evolution.

Considering that hexaquo Mn^{2+} shows a characteristic six-line EPR signal (Yocum et al., 1981; Miller and Brudvig, 1991), release of manganese from its binding site (present in the form of Mn^{2+} symmetrically coordinated by six water molecules) can be measured by EPR spectroscopy. Almost no Mn^{2+} EPR signal was observed in the control (t= 0 min). For increasing heating times, the signal gradually develops; it reaches its maximal amplitude not before 180 min. The increase in the Mn^{2+} EPR signal magnitude is clearly biphasic and the biphasic increase is preceded by a lag phase. The amplitudes of the fast and slow rising component are of equal magnitude (as revealed by curve-fitting) meaning that two of the four protein-bound Mn are released more than ten times faster than the second Mn pair.

The experiments reviewed above demonstrate that:

1) Loss of the oxygen-evolution activity and reduction of Y_D^{ox} occur simultaneously,

2) The disassembly of the Mn complex is associated with the formation of Mn^{2+}.

Results based on EXAFS analysis of the structural rearrangement of the Mn ligand environment triggered by a jump temperature have led to the following conclusions:

- The results of the disassembly process are compatible with the existence of two Mn-Mn vectors of 2.7 Å lengths per Mn_4 complex, suggesting the presence of two pairs of di-μ-oxo-bridge Mn ions in the intact Mn complex in its S_1-state.
- Analysis of EXAFS spectra in control and heated PSII revealed a distance between heavy atoms of ~ 3.3 Å with an apparent coordination number of ~0.5 per Mn which is lost during the most rapid kinetics phase (k_1). The loss of the 3.3 Å distance is not coupled to further structural changes of the Mn complex detectable by EXAFS spectroscopy. Taking into consideration the close relation between Ca and the k_1 process as well as Ca-EXAFS results (Cinco et al., 2004; Yano et al., 2006), calcium likely is at a distance of 3.3 Å to at least two Mn ions.
- The transition to a binuclear Mn complex (k_2 phase) involves reduction of about one-half of the Mn(III,IV) ions to Mn(II).

In summary, in response to a temperature jump, all four Mn atoms are released from their binding site, finally leading to four $[Mn(H_2O)_6]^{2+}$ complexes. One of two di-μ-oxo-bridged Mn pairs is rapidly lost (k_2 = 0.18 min^{-1}), whereas the second Mn pair is much more firmly bound (k_3 = 0.014 min^{-1}). Due to the release of one Ca ion, the reduction and release of any bound Mn is preceded by the rapid loss of a Mn-Ca/Mn vector at 3.3 Å (k_1=1.0 min^{-1}). Whether the Ca release is associated with the release of extrinsic polypeptides, was studied in the present work.

Based on the above results, a kinetic model was constructed (Scheme 1) (Pospisil et al., 2003).

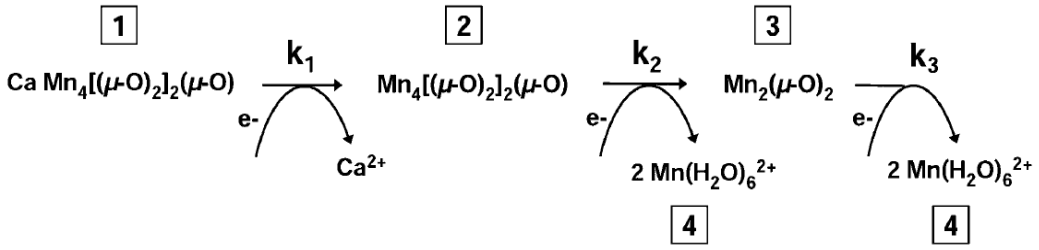

Scheme 1 A kinetic scheme for the stepwise reduction and disassembly of the Mn complex in response to a temperature jump. Four states or intermediates are involved (indicated by the numbers in the squares). The obtained rate constants are k_1 = 1 min^{-1}, k_2 = 0.18 min^{-1} and k_3 = 0.014 min^{-1} (Pospisil et al., 2003).

1.4 Assembly of the catalytic manganese cluster in PSII

1.4.1 Photoactivation

By photoactivation or Photo-assembly (PA), the constituents of the Mn complex (Ca^{2+}, Mn^{2+}, water and possibly bicarbonate and Cl^-) are assembled in the light to form the active site of photosynthetic oxygen evolution activity.

Unlike other metal clusters observed in proteins which undergo spontaneous self-assembly or require proteins (chaperones) for proper formation, the formation of the Mn complex does not require the assistance of chaperones (Ananyev et al., 2001).

In the biological context the photoactivation occurs not only during the *de novo* synthesis of new PSII complexes, it also occurs continuously during PSII repair processing (Suorsa et al., 2004; Chow and Aro, 2005). This is necessary because the susceptibility Mn complex is to the so-called photoinhibition. To overcome the photoinhibition, oxygenic organisms have evolved repair mechanisms permitting a high rate of metabolic turnover of PSII polypeptides, in particular of the D1 protein. Because D1 appears to provide most of the ligands to the Mn complex, the rate of repair-associated photoactivation must follow the D1 protein turnover rate.

A variety of studies have provided insights into the photoactivation process:

- Under in vitro conditions photoactivation requires the PSII apo-protein complex comprising at least the D1/D2 core proteins and the intrinsic antenna CP47 (Buchel et al., 1999) as well as Mn^{2+} (Cheniae and Martin, 1971; Miller and Brudvig, 1989), Ca^{2+} (Miller and Brudvig, 1989; Tamura et al., 1989; Chen et al., 1995; Ananyev and Dismukes, 1996b; Ananyev and Dismukes, 1997), Cl^- ions (Miyao and Inoue, 1991a), and possibly bicarbonate (Baranov et al., 2000), an exogenous electron acceptor in the medium (Miyao and Inoue, 1991b), and visible light. Under certain conditions, the assembly may be more effective when complexed Mn is provided in the medium (Bernat et al., 2001; Han et al., 2005; Liu et al., 2006). Photoassembly of the Mn complex has been studied extensively both under continuous illumination and flashing light (Ananyev et al., 2001; Burnap, 2004).

- The time-course of the recovery of O_2 evolution under continuous and intermittent light, has led to a preliminary kinetic model for the assembly of the cluster, involving

sequential light and dark steps of Mn ligation and photo-oxidation (Tamura and Cheniae, 1987; Tamura et al., 1989; Blubaugh and Cheniae, 1992).

1.4.2 Proposed sequences of photoactivation

Based on in vitro studies, several models for the photo-assembly process have been proposed. By studying the time course of the recovery of O_2 evolution activity under continuous and intermittent light and different Mn^{2+} concentrations, early kinetics studies carried out by Cheniae's group (Cheniae and Martin, 1967; Cheniae and Martin, 1970; Cheniae and Martin, 1971; Cheniae, 1972) addressed the mechanism of photoactivation. This group found evidence for a "two quantum model", in which two Mn^{2+} ions sequentially bind to the apo-PSII complex and are photooxidized. Completion of photoactivation was proposed to require binding of two additional Mn^{2+} ions with subsequent photooxidation producing a stable WOC. Binding of the second Mn^{2+} ion was proposed to be the overall rate determining step of photoactivation. This model was further supported by Miller and Brudvig (Miller and Brudvig, 1989; Miller and Brudvig, 1990), who also showed by EPR that the first light-induced intermediate of photoactivation resulted in the disappearance of Mn^{2+} from the solution. They hypothesized that a second intermediate could contain a dimanganese Mn^{2+} - Mn^{3+} center which, although undetected, could be photooxidized in the next light-dependent step to yield Mn^{3+} - Mn^{3+}.

This kinetic "two-quantum series model" (Radmer and Cheniae, 1971), and its derivatives (Tamura and Cheniae, 1987; Miller and Brudvig, 1989; Miyao and Inoue, 1991b; Miyao-Tokutomi and Inoue, 1992; Ananyev and Dismukes, 1996a; Burnap et al., 1996; Zaltsman et al., 1997) do not deviate fundamentally from the original model derived from (Cheniae and Martin, 1971). Nevertheless, information on the molecular structure and oxidation state of the proposed intermediates is still lacking.

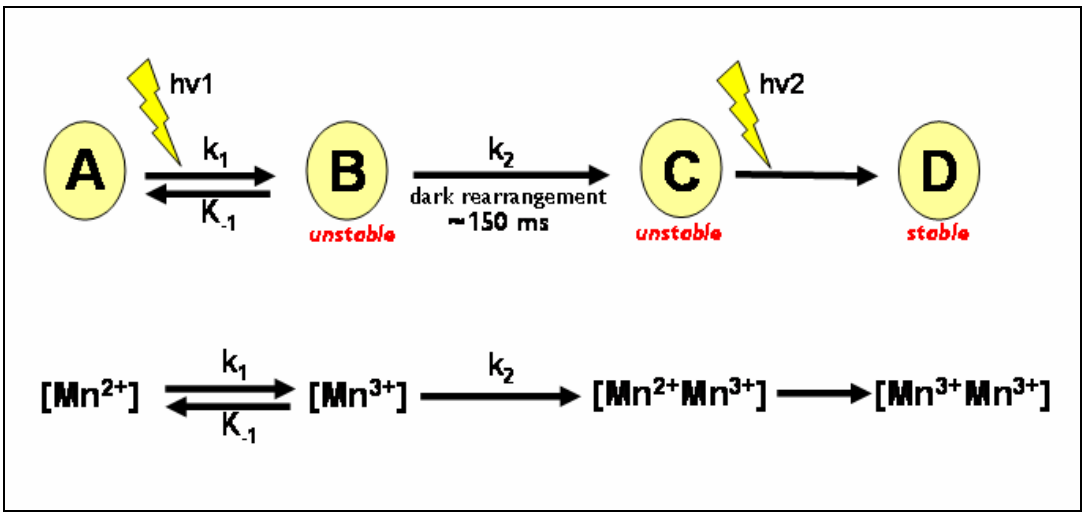

Figure 17 The two-quantum series model involves two steps;
(1) The first photooxidation event, described by (A → B), occurs at the high affinity Mn^{2+} binding site, where a single Mn^{2+} is rapidly oxidized to yield a Mn^{3+} ion with a binding constant of log K_1^{-1} = 5.1. It has recently been shown that titration curves for Mn^{3+} fit well to a single-site-binding model for the Mn^{2+} precursor, characterized by a dissociation constant of k_D= 40 -50 μM at pH=7.5. Directed mutagenesis studies have implicated the D1-Asp170 residue in high affinity binding of the photooxidable Mn^{2+} (Nixon and Diner, 1992; Diner, 2001; Debus et al., 2003), whereas inhibition studies (Ananyev et al., 1999) showed that Mn(II)-OH^+ is the active species that forms upon binding of Mn^{2+} to apo-WOC.
(2) The formation of the intermediate (B), triggers a molecular rearrangement phase (B → C). Regarding this unresolved phase, two alternative models have been proposed. The first model demonstrated two kinetic steps, a slower dark step, which is rate-limiting, and sequentially a fast light step. The dark step and its overall slowness is believed to involve a slow folding of the protein to produce a conformational change. When the Ca^{2+} is not bound to its effectors site (low Ca^{2+} concentration), this dark step showed an increase in its binding affinity (Zaltsman et al., 1997). Whereas during the second step (i.e. under illumination) a second Mn^{2+} binds and oxidizes with a low quantum efficiency to yield a long-lived intermediate containing two Mn^{3+} and Ca^{2+} (Miller and Brudvig, 1989; Tamura et al., 1989; Ono, 2001). On the other hand, a second model postulated that this dark step proceed via an unstable intermediate which contains one Mn^{3+} and one Mn^{2+} denoted by (C) (Tamura and Cheniae, 1987; Miller and Brudvig, 1989; Ono, 2001). The photochemical events themselves, such as photooxidation of bound Mn^{2+}, are intrinsically rapid. However, the initial intermediate form and decay many time before advancing to the next stable intermediate. Thus, the overall slowness of the dark step was explained by the low quantum efficiency of the reaction (Ono and Inoue, 1987; Miller and Brudvig, 1989). The binuclear intermediate Mn^{3+}–Mn^{2+} is unstable and needs a flash of light to photooxidize it to form the first stable intermediate (D), which supposed to be Mn^{3+}–Mn^{3+}. Finally, binding and ligation of another two Mn^{2+} atoms occurs to complete the tetrapolynuclear Mn complex (Burnap, 2004).

1.4.3 The role of calcium in the photoactivation

Extensive studies have attempted to elucidate the role of Ca^{2+} in photoassembly, but the function of this cofactor in assembly and activity remains still unclear.

On the one hand, the binding of one Ca^{2+} ion is required for oxygen evolution in the functional WOC (for reviews, see (Yocum, 1991; Debus, 1992; Andreasson et al., 1995)). Therefore, Ca^{2+} must bind to PSII at some step of the photoactivation process. On the other hand, whether binding of Ca^{2+} is essential for the assembly of the Mn_4 cluster remains a controversial issue. Ono and Inoue (Ono and Inoue, 1983a; Ono and Inoue, 1983b) have proposed that both Mn^{2+} and Ca^{2+} should be bound to their specific sites in order for

photoactivation to occur. However, according to work performed at high Mn^{2+} concentrations, Ca^{2+} is not required for the assembly of the tetramanganese cluster, but only for oxygen evolution itself (Miller and Brudvig, 1989; Tamura et al., 1989). Ananyev and Dismukes (Ananyev and Dismukes, 1996b; Ananyev and Dismukes, 1996a), directly demonstrated, using near-stoichiometric concentrations of Mn^{2+}, that preassembly of an intermediate prior to the active cluster requires the presence of Ca^{2+}.

The binding of one calcium ions has been kinetically resolved during the assembly of the Mn_4 cluster and found to be essential for expression of O_2 evolution activity upon photoactivation (Zaltsman et al., 1997).

Without Ca^{2+}, the apo-WOC-PSII protein may be able to bind and photo-oxidize more than the usual four Mn^{2+} ions (<10 Mn) and fails to aquire oxygen evolution activity (Chen et al., 1995; Zaltsman et al., 1997).

Several roles for the Ca^{2+} in photoactivation have been proposed, including stabilization of photoactivation intermediates (Miller and Brudvig, 1989) and facilitating conformational changes accompanying the rate limiting step (Chen et al., 1995). However, no direct support for either of these roles was provided. It has been shown that in the presence of high concentrations of Mn^{2+} in the medium, Ca^{2+} prevents binding and photooxidation of nonspecific (excess) manganese ions, which diminish the yield of active centers (Chen et al., 1995). However, Calcium may be required for a conformational activation of the tetramanganese cluster (Chen et al., 1995). Ca^{2+} was also shown to slow the overall rate of photoactivation by competing with Mn^{2+} for its binding site(s) (Ono and Inoue, 1983a; Ono and Inoue, 1983b; Hsu et al., 1987; Tamura and Cheniae, 1987; Miller and Brudvig, 1989). Maintenance of an optimal concentration ratio of Mn^{2+} and Ca^{2+} in the photoactivation medium has been shown to be essential to avoid excessive photoinhibition. It has been suggested that Mn^{2+} occupying the Ca^{2+} binding site is prone to photooxidation and subsequent coordination to sites where it impairs the formation of an active WOC (Miller and Brudvig, 1989; Chen et al., 1995).

1.5 Objectives of this thesis

In the first part of this study, I used polarography, SDS gel electrophoresis, EPR spectroscopy, atomic absorption spectroscopy (AAS), delayed and prompt fluorescence, and X-ray absorption spectroscopy (XAS) measurements to investigate the time course of the disassembly of the Mn complex by a temperature jump, in order to obtain insights into the structural organization of the complex and the individual roles of its components, as well as to determine the molecular basis of the heat sensitivity of the water-oxidizing complex.

It was studied:

(1) how the binding of the extrinsic proteins is affected by exposure to an elevated temperature;

(2) whether Mn(II) formed during prolonged heating is released into the bulk;

(3) up to which point electron transfer at the donor side still occurs in PSII samples exposed to 47°C for distinct heating periods (ranging from 0 to 180 min).

In previous investigations it remained unclear whether the intermediates, which were formed during the heat-induced disassembly process, represent models of the partially assembled Mn complex. Therefore in the second part of this study, I have investigated the heat-induced disassembly and subsequent reassembly of the Mn complex by photoactivation. The restoration of the oxygen evolving activity was monitored by polarography and recombination chlorophyll fluorescence. Oxidation state and structural features of the formed intermediates of the Mn complex were assayed by X-ray absorption spectroscopy at the Mn K-edge.

It was studied:

(1) whether the heat-treated PSII is able to act as the starting material for reassembly at various disassembly stages;

(2) whether the Mn^{II} released to the suspending medium by heat treatment, corresponds to the Mn(II) ions reincorporated into the complex by the photoactivation process;

(3) whether there are intemediates formed and whether these are stable;

(4) whether distinct structural motifs are present in a Mn_2 assembly intermediate information and can be identified by X-ray absorption spectroscopy.